Soft Switching Symmetric Bipolar Outputs DC-Transformer (DCX) for Eliminating Power Supply Pumping of Half Bridge Class-D Audio Amplifier

Xiang Zhou, *Member, IEEE*, Jianping Xu, *Member, IEEE*, Shu Zhong and Yan-Fei Liu, *Fellow, IEEE*

Abstract

A soft switching symmetric bipolar outputs DC-transformer (DCX) for eliminating power supply pumping of half bridge class-D audio amplifiers is proposed in this paper. Compared with traditional unidirectional front-end DC-DC converter in half bridge class-D audio amplifier, output capacitances of the proposed DCX and voltage stress of half bridge class-D audio amplifier are significantly reduced. Soft switching of the proposed DCX can be achieved when the load current of half bridge class-D audio amplifier is positive or negative. Thus, the efficiency and power density of the proposed audio amplifier system can be improved. In addition, the proposed DCX has smoothing transition between positive load current and negative load current with simple open-loop controller. The operating principle of the proposed DCX is analyzed and a 200W prototype is built up. Experimental results show that power supply pumping is reduced with small DCX output capacitors, symmetric bipolar outputs are obtained and peak efficiency of 96.3% is achieved.

Index Terms

soft switching, DC-transformer, symmetric bipolar outputs, half bridge class-D audio amplifier

I. Introduction

ALONG with the development of portable audio electronics equipment, audio amplifier with low output voltage distortion, high efficiency and high power-density has attracted much attention recently. Class-D audio amplifiers are thus more and more popular and start to flourish in applications where linear amplifiers once dominated [1]. Compared with linear amplifiers, modern class-D audio amplifiers benefit from small volume and high system efficiency [2].

Class-D audio amplifier can be classified into half bridge and full bridge class-D audio amplifier. Compared with full bridge class-D audio amplifier, half bridge class-D audio amplifier has reduced devices number and stray inductance [3]. In order to provide stable power supply for half bridge class-D audio amplifier system, high performance front-end DC-DC converter is required [4]. Boost converter is used as front-end DC-DC converter to provide unipolar supply for half bridge class-D audio amplifier in [5]. However, a large dc blocking capacitor is required to prevent the speaker from being damaged by high dc voltage, which reduced the power density of the audio amplifier system [6]. In contrast, in half bridge class-D audio amplifier with bipolar power supplies, bulky blocking capacitor can be removed [6]-[7]. Typical half bridge class-D audio amplifier system consists of

front-end single input bipolar outputs DC-DC converter and half bridge class-D audio amplifier. Bipolar outputs flyback converter or *LLC* resonant converter is widely used as front-end converter [8]-[9]. A voltage doubler rectified boost-integrated half bridge class-D audio amplifier is proposed in [10], which achieves ZVS of switches and has no dc magnetizing current for the transformer.

Generally, due to AC load current and traditional unidirectional front-end DC-DC converter, the voltages across power supplies of half bridge class-D audio amplifier have large voltage ripples, especially when output voltage frequency is low, which is called power supply pumping [4]. Severe power supply pumping significantly increases the voltage stress of the devices of class-D audio amplifier and deteriorates total harmonic distortion and noise (THD+N) of the audio amplifier system [11]-[12]. In order to improve THD+N and suppress power supply pumping, some control strategies are studied to obtain high power supply rejection ratio (PSRR) [13]-[15]. In general, large bulky electrolytic capacitor is used as the filter of the front-end DC-DC converter to reduce supply voltage ripple of half bridge class-D audio amplifier system, which reduces the power density of the audio amplifier system.

Compared with large bulky electrolytic capacitor in unidirectional front-end DC-DC converter, bidirectional front-end DC-DC converter can transfer feedback energy to input power supply of the audio amplifier system, which reduces the output capacitor of DC-DC converter and increases the power density [16]. In bidirectional DC-DC converter, soft switching and bidirectional power conversion can be achieved with some control strategies [17]-[21]. However, these converters are controlled to operate in forward operation mode or backward operation mode respectively. As load current of class-D audio amplifier varies rapidly and randomly, which makes it difficult to realize soft switching by detecting the direction of the load current. Thus, these bidirectional soft switching DC-DC converters are not suitable for class-D audio amplifier system.

As a good candidate for front-end DC-DC converter, *LLC* resonant converter attracts much attention in decades. There are many researches on the control, common noise and magnetics design of *LLC* converter [22]-[26]. However, due to complex control algorithm, these converters require microcontroller to achieve start-up and other control functions. In bidirectional soft switching *LLC* DC-DC converter, some control strategies and circuit topologies are designed for soft switching of all the switches in forward or backward mode as well as smooth change of the output power flow direction [27]-[29]. Because maximum output frequency of audio amplifier is 20kHz, it is difficult to design the controller of bidirectional *LLC* converter for audio amplifier system.

In class-D audio amplifier system, because the downstream class-D audio amplifier is close-loop and always has high PSRR, the front-end DC-DC converter can be designed as an open-loop DC-transformer (DCX) to improve the efficiency and reduce complexity of the controller. Light load efficiency and optimized magnetic component of the *LLC* DCX are focus in [30]-[35]. A family of resonant DCX is proposed in [36], which achieve soft switching of switches and high system efficiency over wide load range. However, it is difficult to realize soft switching of all the switches in both forward and backward mode because these DCXs are open-loop and has fixed switching frequency as well as fixed duty cycle.

In this paper, a soft switching symmetric bipolar outputs DCX for eliminating power supply pumping of half bridge class-D

audio amplifier is proposed. Power supply pumping of half bridge class-D audio amplifier is eliminated by the proposed DCX with small output capacitances, thus power supply noise and voltage stress of the devices in the half bridge class-D audio amplifier are reduced. The proposed DCX has stable symmetric bipolar outputs with simple open-loop controller, which significantly reduces complexity of controller in half bridge class-D audio amplifier system. Soft switching of the switches in the proposed DCX can be realized when the load current of half bridge class-D audio amplifier is positive or negative, which improves the system efficiency.

This paper is organized as following. Section II illustrates power supply pumping and circuit configuration of the proposed DCX. Section III gives the analysis of operation modes and performance of the proposed DCX. Section V and VI give experimental results and conclusion.

II. Power Supply Pumping and Topology Derivation of the Proposed DCX

The proposed audio amplifier system, as shown in Fig. 1, consists of front-end DCX and downstream class-D audio amplifier. The proposed DCX has bidirectional power flowing path. Thus, the power supply pumping of half bridge class-D can be reduced since a current path is provided for the reverse load current.

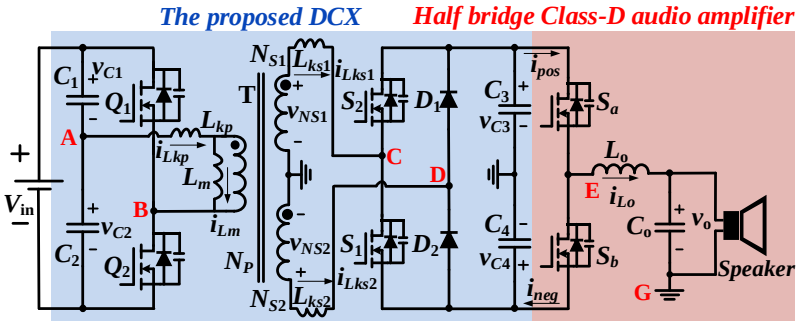

Fig. 1. Circuit diagram of the proposed audio amplifier system

A. *Power supply pumping of half bridge class-D amplifier*

Fig. 2 shows impedance of the speaker versus output voltage frequency of audio amplifier. It can be observed that speaker load can be resistive, capacitive or inductive under different output voltage frequency.

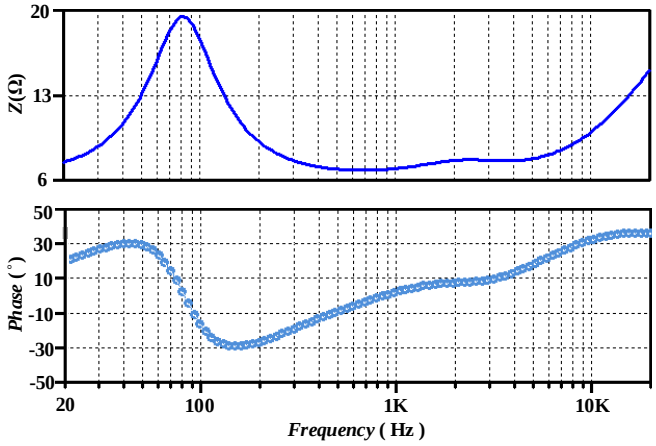

Fig. 2. The typical impedance of speaker versus different output voltage frequency of audio amplifier

Fig. 3 shows half bridge class-D audio amplifier with unidirectional front-end DC-DC converter, and the load is assumed as

resistor. Due to unidirectional power flowing paths, the reverse load current would cause output voltage pumping of the front-end DC-DC converter. Such voltages pumping increases voltage stress of switches S_a, S_b as well as capacitors C_{pos}, C_{neg}, and deteriorates the power supply noise of half bridge class-D audio amplifier.

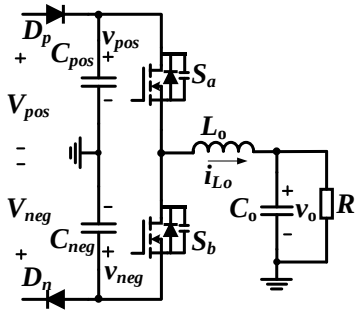

Fig. 3. Half bridge class-D audio amplifier with unidirectional front-end DC-DC converter

Fig.4 illustrates the power supply pumping of the half bridge class-D audio amplifier system as shown in Fig. 3 with resistor load. In Fig. 4(a), i_o is load current of the half bridge class-D audio amplifier, v_{ref} is audio reference voltage, and v_c is carrier. The driving signals of switches S_a and S_b are complementary, T_a is the time when load current is negative and T_b is the time when load current is positive.

For negative load current i_o, when switch S_a is turned on and switch S_b is turned off, load current i_o flows from filter inductor L_o into capacitor C_{pos} through switch S_a. Thus, the charge is stored in capacitor C_{pos}, which causes bus pumping on positive power supply of the class-D audio amplifier. Because voltage v_{pos} is higher than positive power supply voltage V_{pos}, diode D_p is turned off. When switch S_b is turned on and switch S_a is turned off, load current i_o flows from filter inductor L_o into diode D_n through switch S_b. Thus, the negative power supply of the class-D audio amplifier provides power for the load.

For positive load current i_o, when switch S_b is turned on and switch S_a is turned off, load current i_o flows from switch S_b into filter inductor L_o. Thus, the charge is stored in capacitor C_{neg}, which causes bus pumping on negative power supply of the class-D audio amplifier. Because voltage v_{neg} is lower than negative power supply voltage V_{neg}, diode D_n is turned off. When switch S_a is turned on and switch S_b is turned off, load current i_o flows from diode D_p into filter inductor L_o through switch S_a. Thus, the positive power supply of the class-D audio amplifier provides power for the load.

As shown in Fig. 4(a), yellow area represents the time when load current i_o is negative and flows into capacitor C_{pos} through switch S_a. Red area represents the time when load current i_o is positive and flows into C_{neg} through switch S_b. Green and purple areas represent the time when positive and negative power supply provide output power for the load through switches S_a and S_b, respectively. It can be observed that the time of green area is longer than the time of yellow area and the time of purple area is longer than the time of red area.

In Fig. 4(b), V_{pos} and V_{neg} are positive and negative bus voltage for class-D audio amplifier, and Δv_{pos} and Δv_{neg} are positive and negative bus pumping voltage. As shown in Fig. 4(b), when load current i_o is positive and switch S_a is turned on, the charge stored

in capacitor C_{pos} is discharged to provide output power for the load. Thus, during the time interval t_4~t_5, voltage v_{pos} decreases from the maximum to positive bus voltage V_{pos}. When load current i_o is negative and switch S_b is turned on, the charge stored in capacitor C_{neg} is discharged to provide output power for the load. Thus, during the time interval t_2~t_3, voltage v_{neg} increases from the minimum to negative bus voltage V_{neg}.

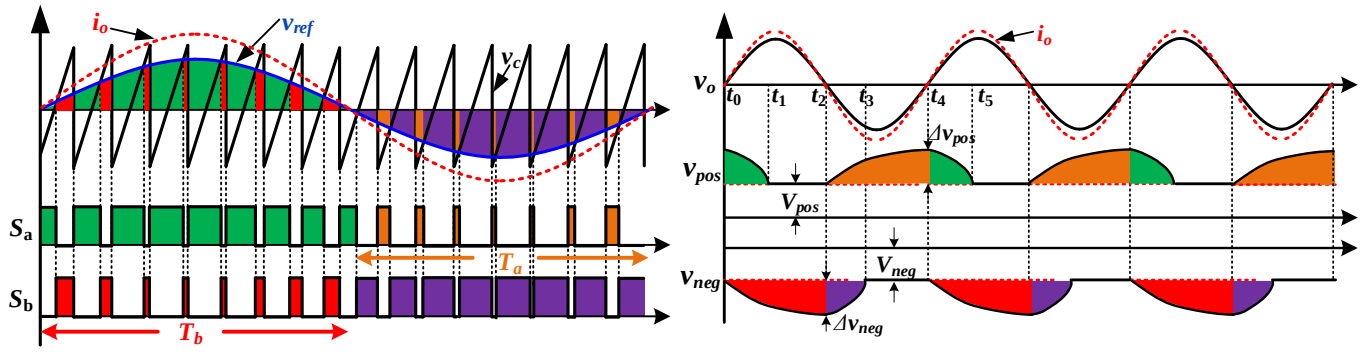

(a) key waveforms of half bridge class-D audio amplifier (b) power supply pumping of half bridge class-D audio amplifier system

Fig. 4. Power supply pumping of half bridge class-D audio amplifier with unidirectional front-end DC-DC converter under resistor load

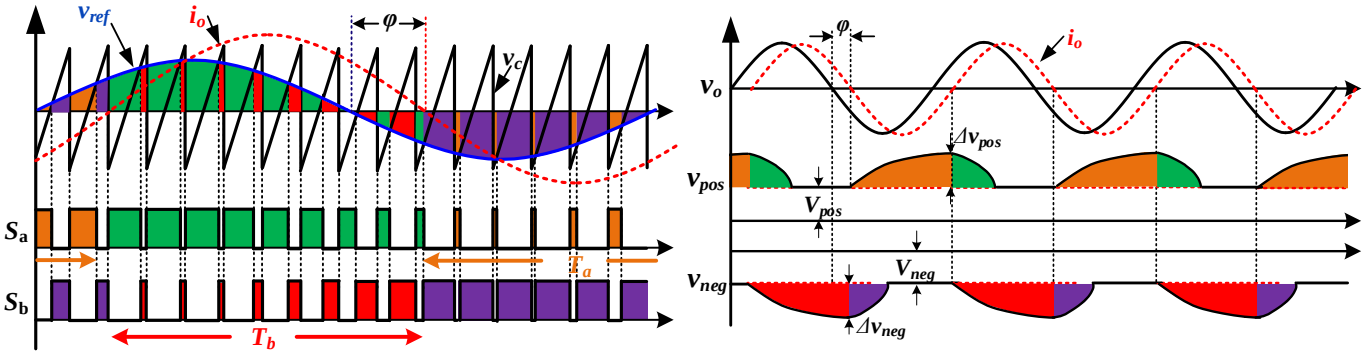

(a) key waveforms of half bridge class-D audio amplifier (b) power supply pumping of half bridge class-D audio amplifier system

Fig. 5. Power supply pumping of half bridge class-D audio amplifier with unidirectional front-end DC-DC converter under inductive load

When the speaker load of audio amplifier is inductive or capacitive, load current i_o in Fig. 4(a) will shift to right or left. Fig. 5 illustrates the power supply pumping of the half bridge class-D audio amplifier system as shown in Fig. 3 with inductive load. With inductive or capacitive load, when load current i_o is negative and switch S_a is turned on, the time of yellow area is longer than that with resistive load, which causes more severe bus pumping on capacitor C_{pos}. Similarly, when load current i_o is positive and switch S_b is turned on, the time of red area is longer than that with resistive load, which causes more severe bus pumping on capacitor C_{neg}. The analysis of power supply pumping of the half bridge class-D audio amplifier system with inductive load is similar to that with resistive load.

In order to calculate the power supply pumping of half bridge class-D audio amplifier, setting

$$\begin{cases} v_o = mV_{bus}\sin(\omega t) \\ i_o = \dfrac{mV_{bus}\sin(\omega t+\varphi)}{\left|Z_{speaker}\right|} \end{cases}. \tag{1}$$

where m is modulation index of class-D audio amplifier, V_{bus} is power supply voltage of the class-D audio amplifier, which equals to the magnitude of V_{pos} and V_{neg}, ω is angular frequency of output voltage of audio amplifier, φ is phase difference which the output current lags output voltage of audio amplifier, and $Z_{speaker}$ is impedance of the speaker.

In the half bridge class-D audio amplifier, the duty cycle of switch S_a is

$$d_{Sa} = \frac{1}{2} + \frac{1}{2} m \sin(\omega t). \tag{2}$$

As shown in Fig. 5, during T_a, load current i_o flows into capacitor C_{pos} through switch S_a, which increases the voltage across capacitor C_{pos}. If switching frequency and output voltage frequency of the class-D audio amplifier satisfy f_s: f_o =N, the voltage ripple across positive power supply Δv_{pos} satisfy

$$\begin{aligned} C_{pos} \cdot \Delta v_{pos} &= \int_{\frac{\pi-\varphi}{\omega}}^{\frac{2\pi-\varphi}{\omega}} -i_{Sa}(t)dt \\ &= \sum_{i=N/2}^{N} \{-\frac{mV_{pos}}{|Z_{speaker}|} \sin(\frac{\omega i}{N} + \varphi) \cdot [\frac{1}{2} + \frac{1}{2} m \sin(\frac{\omega i}{N})]\}. \end{aligned} \tag{3}$$

When $N \to +\infty$, equation (3) can be rewritten as

$$\begin{aligned} C_{pos} \cdot \Delta v_{pos} &= \int_{\pi}^{2\pi} -\frac{mV_{pos}}{\omega |Z_{speaker}|} \sin(x)[\frac{1}{2} + \frac{1}{2} m \sin(x-\varphi)]dx \\ &= \frac{mV_{pos}(4 - m\pi\cos\varphi)}{4\omega |Z_{speaker}|}. \end{aligned} \tag{4}$$

Therefore, the ripple voltage across positive power supply is

$$\Delta v_{pos} = \frac{mV_{pos}(4 - m\pi\cos\varphi)}{8\pi f_o |Z_{speaker}| C_{pos}}. \tag{5}$$

Similarly, the ripple voltage across negative power supply is

$$\Delta v_{neg} = \frac{mV_{pos}(4 - m\pi\cos\varphi)}{8\pi f_o |Z_{speaker}| C_{neg}}. \tag{6}$$

It can be observed from equations (5)-(6) that when output voltage frequency of audio amplifier is low, power supply pumping is severe. Assume that m=0.7, V_{pos}=35V, Z_{load}=4Ω and φ=π/6, according to equations (5)-(6), Fig. 6 shows the relationship between Δv_{pos}=Δv_{neg} and capacitances C_{pos}=C_{neg}. As shown in Fig. 6, if f_o=20Hz, Δv_{pos}=Δv_{neg}=35V, large capacitors C_{pos}=C_{neg}=731.1μF with 70V voltage stress are needed. If smaller voltage ripple Δv_{pos}=Δv_{neg} is required, it has to increase capacitances C_{pos}=C_{neg}, which reduces power density of the audio amplifier system.

If the diodes D_p and D_n in Fig. 3 are replaced by switches and bidirectional current flowing path is provided for half bridge class-D audio amplifier, the charge can be transferred instead of stored in the capacitors C_{pos} and C_{neg}, thus power supply pumping can be eliminated.

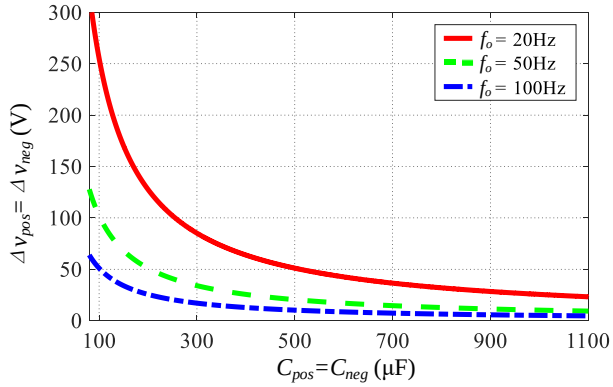

Fig. 6. Voltage ripple $\Delta v_{pos}=\Delta v_{neg}$ versus capacitances $C_{pos}=C_{neg}$

B. *Topology derivation of the proposed DCX*

Half bridge circuit, full bridge circuit, push-pull circuit, two-switch forward circuit, etc, can be used in transformer primary to generate square wave voltage with 0.5 duty cycle. Fig. 7 shows circuit configuration of the proposed DCX. When square wave with constant duty cycle is generated in transformer primary, the proposed DCX can generate constant positive and negative output voltages when full wave or full bridge rectifier is adopted in transformer secondary. Thus, if the leakage inductance of the transformer is neglected, the bipolar output voltages of the proposed DCX are always clamped by the input voltage of the DCX. Therefore, the voltage ripples across outputs of the proposed DCX are theoretically zero, even if output capacitors of the DCX are zero. Thus, output filter of the DCX is reduced, and the power density of the proposed audio amplifier system can be improved.

In Fig. 7, in order to generate symmetric bipolar outputs, two full bridge rectifiers are necessary to ensure constant output voltages in type I DCX, as shown in Fig. 7(a). Compared with type II DCX as shown in Fig. 7(b), type I DCX needs more rectifier diodes or switches. Thus, type II DCX with half bridge circuit in transformer primary is adopted.

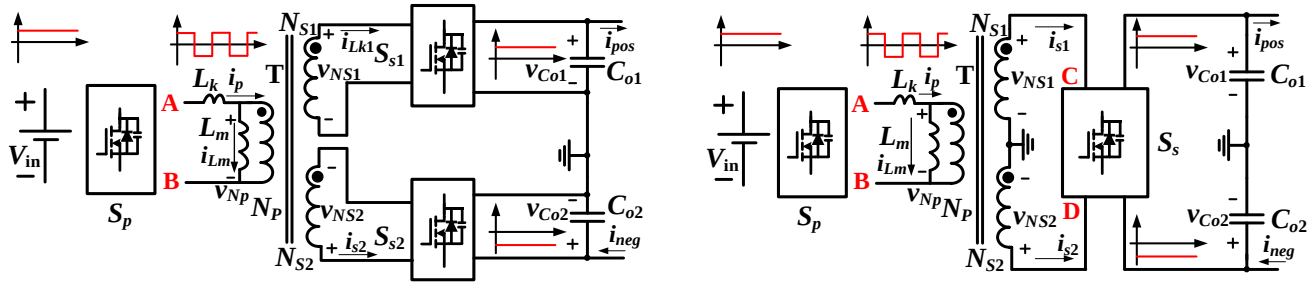

(a) Type I (b) Type II

Fig. 7. Circuit configuration of the proposed DCX

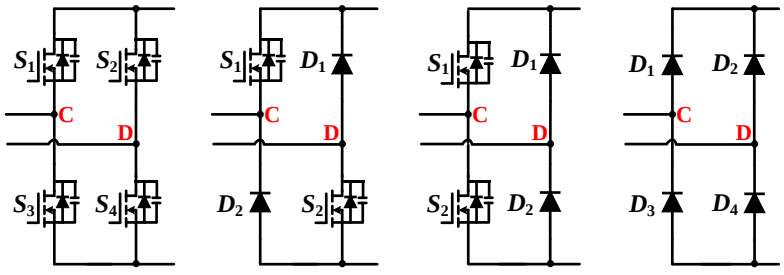

(a) (b) (c) (d)

Fig. 8. Circuit diagram of rectifier

Fig. 8 shows four kinds of rectifier. Front-end bidirectional DC-DC converter is required to reduce power supply pumping in half bridge class-D audio amplifier and provide a path for the reserve load current. The rectifier as shown in Fig. 8(c) is adopted in the proposed DCX due to bidirectional power conversion with less active devices.

III. Analysis of Operation Modes and Characteristic of the Proposed DCX

In this paper, the proposed DCX is connected to half bridge class-D audio amplifier. For audio amplifier, the load current is AC and the frequency range of load current is 20Hz~20kHz, which is much lower than the switching frequency of the proposed DCX. Therefore, in one switching period of the proposed DCX, the load current of the half bridge class-D audio amplifier can be regard as constant since filter inductor is large and ripple current of filter inductor is small.

Fig. 9 shows the circuit diagram of power flow in the proposed DCX. As shown in Fig. 9(a), for negative load current, when switch S_a is turned on, current i_{load} flows from switch S_a to capacitor C_3 and positive bus is charged. Therefore, the power is returned to positive bus. As shown in Fig. 9(b), for negative load current, when switch S_b is turned on, current i_{load} flows from switch S_b to capacitor C_4. Therefore, the power is consumed by the load. As shown in Fig. 9(c), for positive load current, when switch S_a is turned on, current i_{load} flows from capacitor C_3 to switch S_a. Therefore, the power is consumed by the load. As shown in Fig. 9(d), for positive load current, when switch S_b is turned on, current i_{load} flows from capacitor C_4 to switch S_b and negative bus is discharged. Therefore, the power is returned to negative bus.

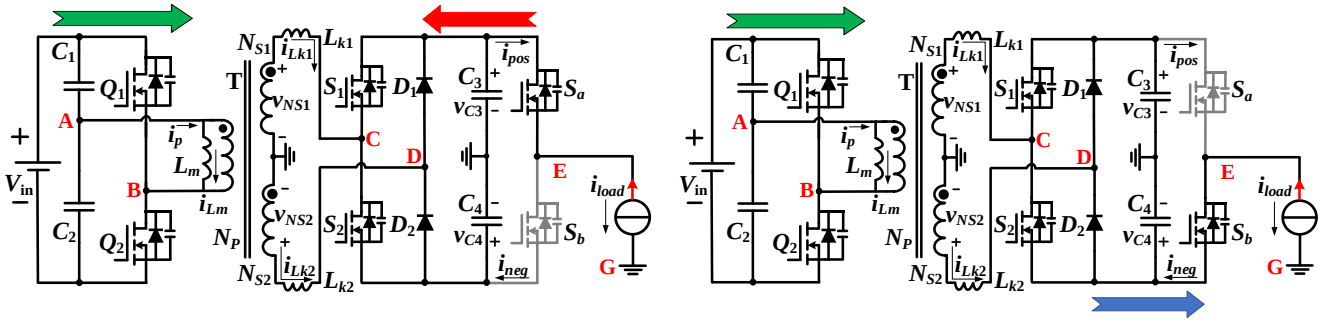

(a) negative load current of class-D audio amplifier when switch S_a is turned on

(b) negative load current of class-D audio amplifier when switch S_b is turned on

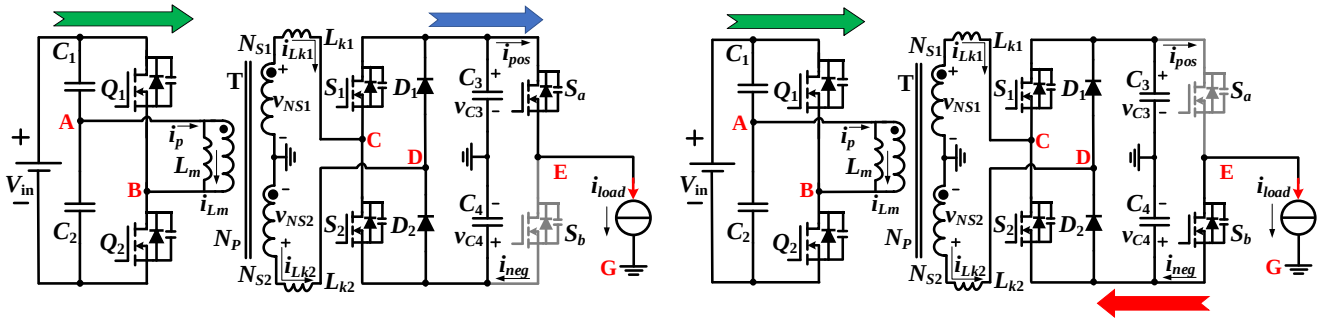

(c) positive load current of class-D audio amplifier when switch S_a is turned on

(d) positive load current of class-D audio amplifier when switch S_b is turned on

Fig. 9. Circuit diagram of power flow in the proposed DCX

As shown in Fig. 5(a), if -90°<φ<90°, the time of green area is longer than the time of yellow area, and the time of purple area is longer than the time of red area, which means that the conduction time of switch S_b is longer than that of switch S_a when current i_{load} is negative, and the conduction time of switch S_a is longer than that of switch S_b when current i_{load} is positive. Thus, the average power of the proposed DCX is positive when load current is positive or negative. In the proposed DCX, positive and negative outputs have bidirectional power, input port has unidirectional power. For positive output, the feedback energy can be consumed by the negative output, and for negative output, the feedback energy can be consumed by the positive output.

In order to ensure low-distortion of output voltage at 20kHz or even higher audio signal frequency, the switching frequency of class-D audio amplifier is generally very high. As the switching frequency of class-D audio amplifier is higher than the switching frequency of the proposed DCX, when the operation mode of the proposed DCX is analyzed, the load current can be regards as two average equivalent current sources for positive and negative bus. The average equivalent current sources $i_{load,p}$ and $i_{load,n}$ satisfy

$$\begin{cases} i_{load,p}(t) = d_{Sa} i_{load} = d_{Sa} i_o \\ i_{load,n}(t) = d_{Sb} i_{load} = d_{Sb} i_o . \end{cases} \tag{7}$$

From equations (1)-(2) and (7), average equivalent current sources $i_{load,p}$ and $i_{load,n}$ are

$$\begin{cases} i_{load,p}(t) = [\frac{1}{2} + \frac{1}{2} m \sin(\omega t)] \frac{m V_{bus} \sin(\omega t + \varphi)}{|Z_{speaker}|} \\ i_{load,n}(t) = -[\frac{1}{2} - \frac{1}{2} m \sin(\omega t)] \frac{m V_{bus} \sin(\omega t + \varphi)}{|Z_{speaker}|} . \end{cases} \tag{8}$$

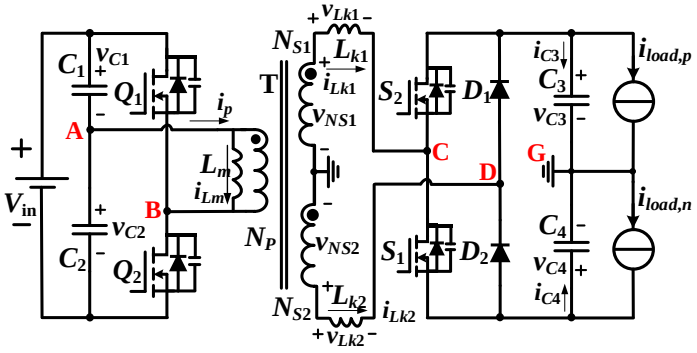

Fig. 10. Equivalent circuit of the proposed DCX

In order to simplify the analysis of the proposed DCX as shown in Fig.2, assume that all power switches are ideal except their body diode and output capacitances C_{oss}, the output capacitances of all switches are the same, and the diodes are ideal. Fig. 10 shows the equivalent circuit of the proposed DCX connected half bridge class-D audio amplifier.

A. *Operation modes of the proposed DCX when load current of class-D audio amplifier is positive*

When load current of half-bridge class-D audio amplifier is positive, currents $i_{load,p}$ and $i_{load,n}$ satisfy $i_{load,p}$>0 and $i_{load,n}$<0 in the equivalent circuit of the proposed DCX. Fig. 11 shows the key waveforms of the proposed DCX. As shown in Fig. 11, t_{d1} and t_{d2} are the dead time of primary side half bridge circuit. If t_{d1} and t_{d2} are neglected, the driving signals of switches Q_1 and Q_2 are

complementary with constant duty cycle 0.5. In order to ensure soft switching of switches S_1-S_2, the turn-on of switches S_1 and S_2 should lag behind the turn-on of switch Q_1 and Q_2 with a delay time t_{d3} and t_{d4}. If dead time and delay time are neglected, the driving signals of switches S_1 and S_2 are complementary with constant duty cycle 0.5. In steady state, the proposed DCX has seven operation modes as shown in Fig. 12.

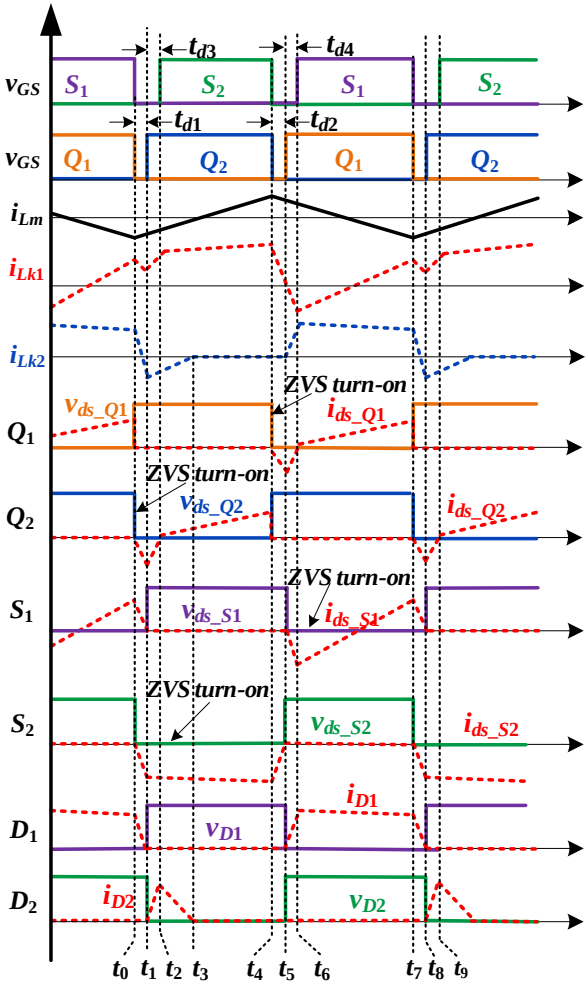

Fig. 11. The key waveforms of the proposed DCX when currents $i_{load,p}$>0 and $i_{load,n}$<0

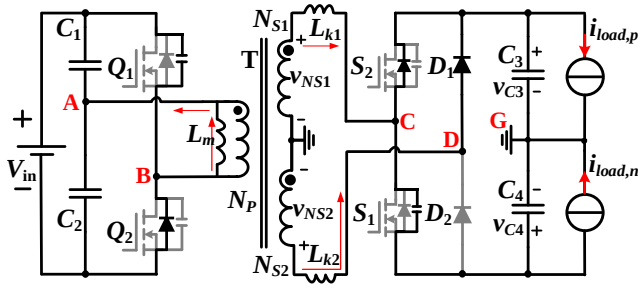

(a) Mode 1 (t_0~t_1)

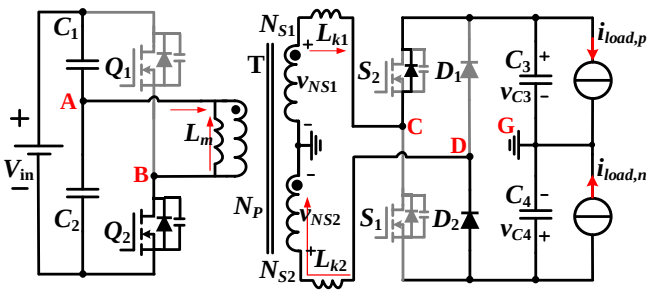

(b) Mode 2 (t_1~t_2)

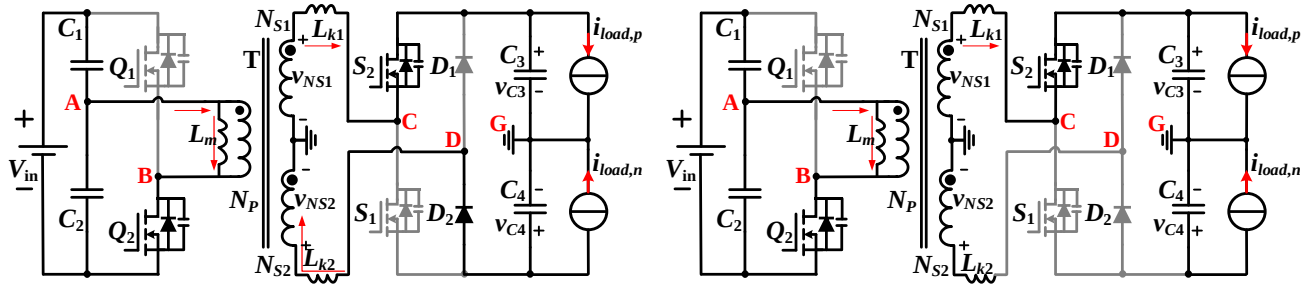

(c) Mode 3 (t_2~t_3)

(d) Mode 4 (t_3~t_4)

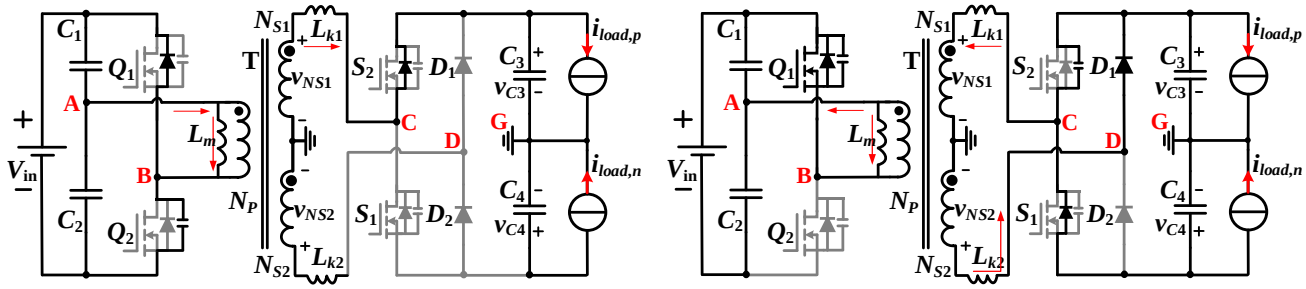

(e) Mode 5 (t_4~t_5)

(f) Mode 6 (t_5~t_6)

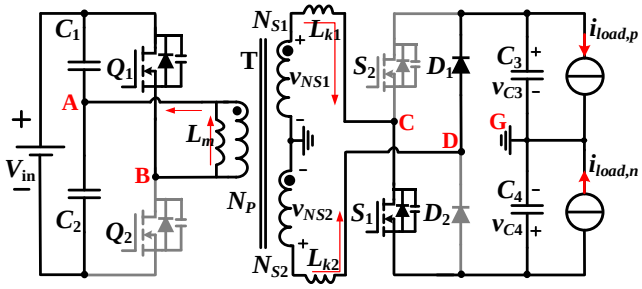

(g) Mode 7 (t_6~t_7)

Fig. 12. Operation mode of the proposed DCX when currents $i_{load,p}$>0 and $i_{load,n}$<0

Mode 1 [t_0~t_1]: At t_0, switches Q_1 and S_1 are turned off, the proposed DCX operates in dead time mode. After switches Q_1 and S_1 are turned off, the output capacitor of switch Q_1 is charged and the output capacitor of switch Q_2 is discharged. Voltage across node A and node B v_{AB} changes from negative to positive, thus current i_{Lk2} decreases. The body diode of switch S_2 is conducted to provide current flowing paths for the freewheeling of secondary leakage inductance current i_{Lk1}. When the output capacitor of switch Q_2 is completely discharged, the body diode of switch Q_2 is conducted and ZVS turn-on of switch Q_2 can be achieved. This mode is short and ends when switch Q_2 is turned on at t_1.

To ensure ZVS turn-on of switch Q_2, it should have

$$\frac{1}{2}\frac{L_{k1}+L_{k2}}{4n^2}[-ni_{Lk1}(t_0)+ni_{Lk2}(t_0)-i_{Lm}(t_0)]^2+\frac{1}{2}L_m i_{Lm}(t_0)^2 > \frac{1}{2}(C_{oss,Q1}+C_{oss,Q2})V_{in}{}^2. \tag{9}$$

It can be observed from (9), L_m is much larger than L_{k1} and L_{k2}, and ZVS turn-on of switch Q_2 can be achieved easily. If ZVS turn-on of switch Q_2 can be achieved in dead time t_{d1}, $t_{d1}=t_1-t_0$ should satisfy

$$\int_{t_0}^{t_1}[-ni_{Lk1}+ni_{Lk2}-i_{Lm}]dt>(C_{oss,Q1}+C_{oss,Q2})V_{in}. \tag{10}$$

Because current i_{Lm} can be regard as constant during t_{d1}, (10) can be approximated and rewritten as

$$-i_{Lm}(t_0)t_{d1}=\frac{V_{in}T}{4L_m}t_{d1}>(C_{oss,Q1}+C_{oss,Q2})V_{in}. \tag{11}$$

Mode 2 [t_1~t_2]: At t_1, switch Q_2 is turned on, and the proposed DCX operates in delay time mode. In this mode, because voltage v_{AB} is positive, current i_{Lk1} is positive and current i_{Lk2} is negative, the body diode of S_2 and diode D_2 are conducted to provide current flowing paths for currents i_{Lk1} and i_{Lk2}. This mode is short and ends when switch S_2 is turned on at t_2.

Mode 3 [t_2~t_3]: At t_2, switch S_2 achieves ZVS turn-on. In this mode, because the load current $i_{load,p}$ is positive and the load current $i_{load,n}$ is negative, the input power supply provides power for positive output through leakage inductance L_{k1} and switch S_2.

In this mode, because the load current $i_{load,n}$ is negative, voltage v_{C4} decreases and is lower than v_{NS2}. Current i_{Lk2} increases from negative to zero, and diode D_2 achieves ZCS turn-off. This mode ends when diode D_2 is turned off at t_3.

Mode 4 [t_3~t_4]: At t_3, diode D_2 is turned off. In this mode, switches Q_2 and S_2 are conducted. Current i_{Lk1} still flows from switch S_2 to capacitor C_3. This mode ends when switches Q_2 and S_2 are turned off at t_4.

Mode 5 [t_4~t_5]: At t_4, switches Q_2 and S_2 are turned off. the proposed DCX operates in dead time mode. After switches Q_2 and S_2 are turned off, the output capacitor of switch Q_2 is charged and the output capacitor of switch Q_1 is discharged. Voltage across node A and node B v_{AB} changes from positive to negative, thus current i_{Lk1} decreases sharply. The body diode of switch S_2 is still conducted when current i_{Lk1} is positive. When the output capacitor of switch Q_1 is completely discharged, the body diode of switch Q_1 is conducted and ZVS turn-on of switch Q_1 can be achieved. This mode is short and ends when switch Q_1 is turned on at t_1.

To ensure ZVS turn-on of switch Q_1, it should have

$$\begin{aligned}\frac{1}{2}\frac{L_{k1}+L_{k2}}{4n^2}[ni_{Lk1}(t_4)+i_{Lm}(t_4)]^2+\frac{1}{2}L_m i_{Lm}(t_4)^2\\ >\frac{1}{2}(C_{oss,Q1}+C_{oss,Q2})V_{in}{}^2.\end{aligned} \tag{12}$$

It can be observed from (12), L_m is much larger than L_{k1} and L_{k2}, and ZVS turn-on of switch Q_1 can be achieved easily. If ZVS turn-on of switch Q_1 can be achieved in dead time t_{d2}, $t_{d2}=t_5-t_4$ should satisfy

$$\int_{t_4}^{t_5}[ni_{Lk1}+i_{Lm}]dt>(C_{oss,Q1}+C_{oss,Q2})V_{in}. \tag{13}$$

Because current i_{Lm} can be regard as constant during t_{d2}, (13) can be approximated and rewritten as

$$i_{Lm}(t_4)t_{d2} = \frac{V_{in}T}{4L_m}t_{d2} > (C_{oss,Q1} + C_{oss,Q2})V_{in}. \quad (14)$$

Mode 6 [t_5~t_6]: At t_5, switch Q_1 is turned on, and the proposed DCX operates in delay time mode. Current i_{Lk1} decreases to negative and current i_{Lk2} is positive. In this mode, the body diode of S_1 and diode D_1 are conducted to provide current flowing paths for currents i_{Lk1} and i_{Lk2}. This mode is short and ends when switch S_1 is turned on at t_6.

Mode 7 [t_6~t_7]: At t_6, switch S_1 achieves ZVS turn-on. Because the load current $i_{load,p}$ is positive and the load current $i_{load,n}$ is negative. In this mode, the input power supply provides power for positive output through leakage inductance L_{k2} and diode D_1.

Because the load current $i_{load,n}$ is negative and capacitor C_4 is discharged in mode 3 as shown in Fig. 12, current i_{Lk1} increases from negative to positive and flows form switch S_1 to capacitor C_4 to balance the charge of capacitor C_4 in this mode. This mode ends when switches Q_1 and S_1 are turned off at t_7.

B. *Operation modes of the proposed DCX when load current of class-D audio amplifier is negative*

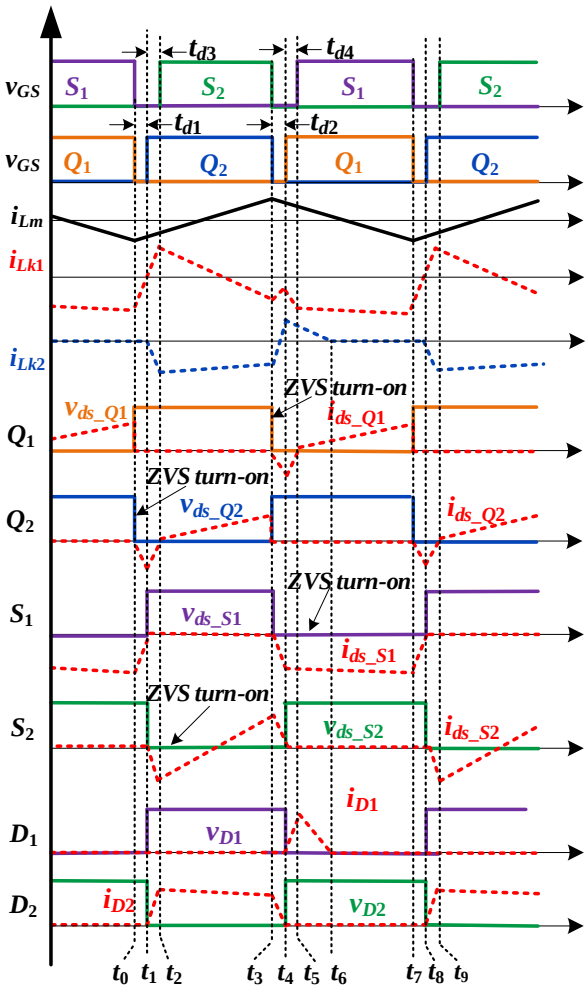

Fig. 13 The key waveforms of the proposed DCX when currents $i_{load,p}$<0 and $i_{load,n}$>0

When load current of half-bridge class-D audio amplifier is negative, currents $i_{load,p}$ and $i_{load,n}$ satisfy $i_{load,p}$<0 and $i_{load,n}$>0 in the equivalent circuit of the proposed DCX. Fig. 13 shows the key waveforms of the proposed DCX. As shown in Fig. 13, t_{d1} and t_{d2}

are the dead time of primary side half bridge circuit. If t_{d1} and t_{d2} are neglected, the driving signals of switches Q_1 and Q_2 are complementary with constant duty cycle 0.5. In order to ensure soft switching of switches S_1-S_2, the turn-on of switches S_1 and S_2 lags behind the turn-on of switch Q_1 and Q_2 with a delay time t_{d3} and t_{d4}. If t_{d3} and t_{d4} are neglected, the driving signals of switches S_1 and S_2 are complementary with constant duty cycle 0.5. In steady state, the proposed DCX has seven operation modes as shown in Fig. 14.

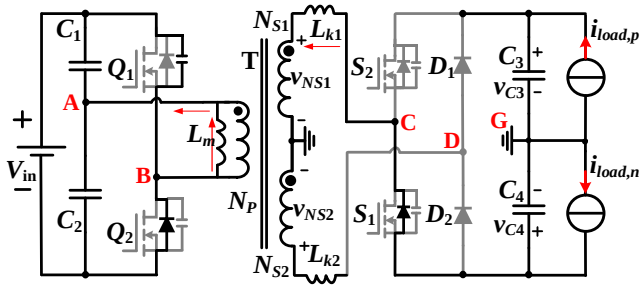

(a) Mode 1 (t_0~t_1)

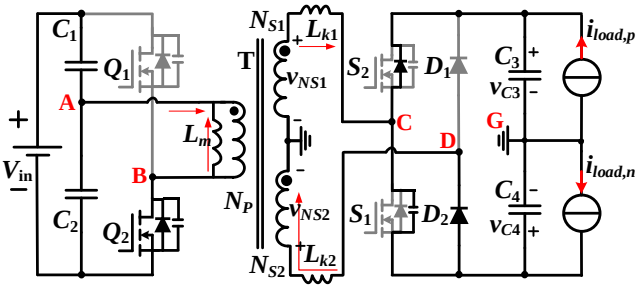

(b) Mode 2 (t_1~t_2)

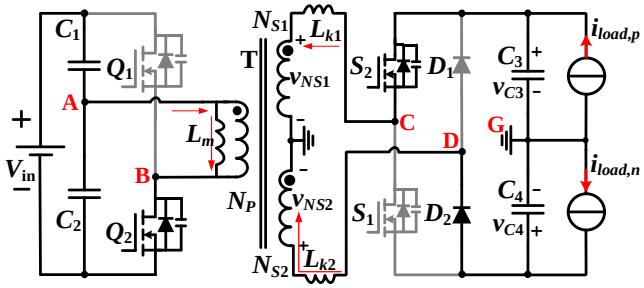

(c) Mode 3 (t_2~t_3)

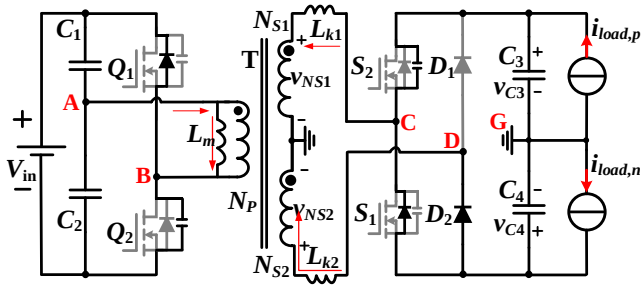

(d) Mode 4 (t_3~t_4)

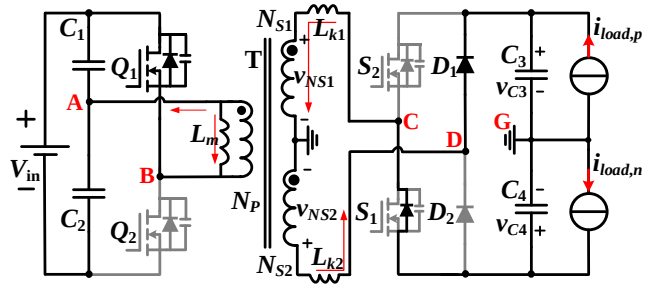

(e) Mode 5 (t_4~t_5)

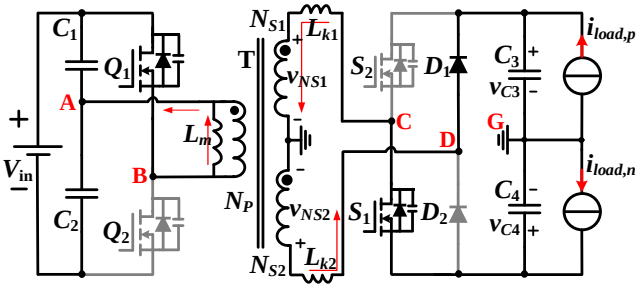

(f) Mode 6 (t_5~t_6)

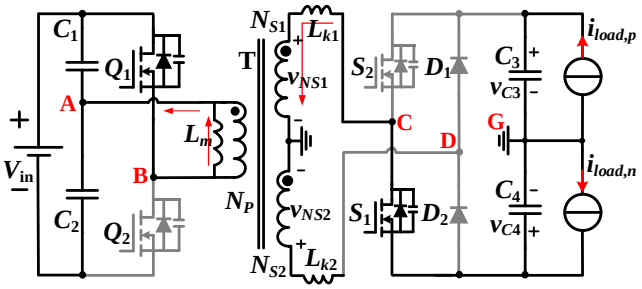

(g) Mode 7 (t_6~t_7)

Fig. 14. Operation mode of the proposed DCX

Mode 1 [t_0~t_1]: At t_0, switches Q_1 and S_1 are turned off, the proposed DCX operates in dead time mode. After switches Q_1 and S_1 are turned off, the output capacitor of switch Q_1 is charged and the output capacitor of switch Q_2 is discharged. Voltage across node A and node B v_{AB} changes from negative to positive, thus current i_{Lk1} increases sharply. The body diode of switch S_1 is still conducted when current i_{Lk1} is negative. When the output capacitor of switch Q_2 is completely discharged, the body diode of switch Q_2 is conducted and ZVS turn-on of switch Q_2 can be achieved. This mode is short and ends when switch Q_2 is turned on at t_1.

To ensure ZVS turn-on of switch Q_2, it should have

$$\frac{1}{2}\frac{L_{k1}+L_{k2}}{4n^2}[-ni_{Lk1}(t_0)-i_{Lm}(t_0)]^2+\frac{1}{2}L_m i_{Lm}(t_0)^2 > \frac{1}{2}(C_{oss,Q1}+C_{oss,Q2})V_{in}{}^2. \tag{15}$$

It can be observed from (15), L_m is much larger than L_{k1} and L_{k2}, and ZVS turn-on of switch Q_1 can be achieved easily. If ZVS turn-on of switch Q_1 can be achieved in dead time t_{d1}, t_{d1}=t_1−t_0 should satisfy

$$\int_{t_0}^{t_1}[-ni_{Lk1}-i_{Lm}]dt > (C_{oss,Q1}+C_{oss,Q2})V_{in}. \tag{16}$$

Because current i_{Lm} can be regard as constant during t_{d1}, (16) can be approximated and rewritten as

$$-i_{Lm}(t_0)t_{d1}=\frac{V_{in}T}{4L_m}t_{d1} > (C_{oss,Q1}+C_{oss,Q2})V_{in}. \tag{17}$$

Mode 2 [t_1~t_2]: At t_1, switch Q_2 is turned on, and the proposed DCX operates in delay time mode. In this mode, because voltage v_{AB} is positive, current i_{Lk1} increases to positive and current i_{Lk2} is negative, the body diode of S_2 and diode D_2 are conducted to provide current flowing paths for currents i_{Lk1} and i_{Lk2}. This mode is short and ends when switch S_2 is turned on at t_2.

Mode 3 [t_2~t_3]: At t_2, switch S_2 achieves ZVS turn-on. In this mode, because the load current $i_{load,n}$ is positive and the load current $i_{load,p}$ is negative, the input power supply provides power for negative output through leakage inductance L_{k2} and diode D_2.

Because the load current $i_{load,p}$ is negative and capacitor C_3 is charged in mode 6 as shown in Fig.14, current i_{Lk1} decreases from positive to negative and flows from capacitor C_3 to switch S_2 to balance the charge of capacitor C_4 in this mode. This mode ends when switches Q_2 and S_2 are turned off at t_3.

Mode 4 [t_3~t_4]: At t_3, switches Q_2 and S_2 are turned off. the proposed DCX operates in dead time mode. After switches Q_2 and S_2 are turned off, the output capacitor of switch Q_2 is charged and the output capacitor of switch Q_1 is discharged. Voltage across node A and node B v_{AB} changes from positive to negative, thus current i_{Lk2} increases sharply. The body diode of S_1 is conducted to provide current flowing paths for currents i_{Lk1} and the diode D_2 is still conducted when current i_{Lk1} is negative. When the output capacitor of switch Q_1 is completely discharged, the body diode of switch Q_1 is conducted and ZVS turn-on of switch Q_1 can be achieved. This mode is short and ends when switch Q_1 is turned on at t_4.

To ensure ZVS turn-on of switch Q_1, it should have

$$\frac{1}{2}\frac{L_{k1}+L_{k2}}{4n^2}[-ni_{Lk1}(t_3)+ni_{Lk2}(t_3)+i_{Lm}(t_3)]^2+\frac{1}{2}L_m i_{Lm}(t_3)^2 > \frac{1}{2}(C_{oss,Q1}+C_{oss,Q2})V_{in}{}^2. \tag{18}$$

It can be observed from (18), L_m is much larger than L_{k1} and L_{k2}, and ZVS turn-on of switch Q_2 can be achieved easily. If ZVS turn-on of switch Q_2 can be achieved in dead time t_{d2}, t_{d2}=t_4−t_3 should satisfy

$$\int_{t_3}^{t_4}[-ni_{Lk1}+ni_{Lk2}+i_{Lm}]dt > (C_{oss,Q1}+C_{oss,Q2})V_{in}. \tag{19}$$

Because current i_{Lm} can be regard as constant during t_{d2}, (19) can be approximated and rewritten as

$$i_{Lm}(t_4)t_{d2}=\frac{V_{in}T}{4L_m}t_{d2} > (C_{oss,Q1}+C_{oss,Q2})V_{in}. \tag{20}$$

Mode 5 [t_4~t_5]: At t_4, switch Q_1 is turned on, and the proposed DCX operates in delay time mode. Current i_{Lk1} is negative and current i_{Lk2} is positive. In this mode, the body diode of S_1 and diode D_1 are conducted to provide current flowing paths for currents i_{Lk1} and i_{Lk2}. This mode is short and ends when switch S_1 is turned on at t_5.

Mode 6 [t_5~t_6]: At t_5, switch S_1 achieves ZVS turn-on. Because the load current $i_{load,p}$ is negative and the load current $i_{load,n}$ is positive. In this mode, the input power supply provides power for negative output through leakage inductance L_{k1} and switch S_1.

In this mode, because the load current $i_{load,p}$ is negative, voltage v_{C3} increases and is higher than v_{NS2}. Current i_{Lk2} decreases from positive to zero, and diode D_1 achieves ZCS turn-off. This mode ends when diode D_1 is turned off at t_6.

Mode 7 [t_6~t_7]: At t_6, diode D_1 is turned off. In this mode, switches Q_1 and S_1 are conducted. Current i_{Lk1} still flows from capacitor C_4 to switch S_1. This mode ends when switches Q_1 and S_1 are turned off at t_7.

C. *Characteristic analysis of the proposed DCX*

In the positive or negative half AC output current cycle of class-D audio amplifier, dead times t_{d1} and t_{d2}, as well as delay times t_{d3} and t_{d4} are very short. If t_{d1}, t_{d2}, t_{d3} and t_{d4} are neglected, according to volte-second balance of L_{k1}, it has

$$\int_0^{\frac{T}{2}}[\frac{nV_{in}}{2}-v_{C3}(t)]=\int_{\frac{T}{2}}^{T}[\frac{nV_{in}}{2}+v_{C4}(t)]. \tag{21}$$

From (21), there is

$$\int_0^{\frac{T}{2}}v_{C3}(t)=-\int_{\frac{T}{2}}^{T}v_{C4}(t). \tag{22}$$

According to equation (22), if voltage ripples across capacitors C_3 and C_4 are small, then the average voltage V_{C3} is equal to $-V_{C4}$. Thus, output voltages of the proposed DCX is symmetric no matter what load current, which is suitable for providing bipolar supplies for half bridge class-D audio amplifier.

As shown in Fig. 15, the current flowing through transformer of *LLC* DC-DC converter and the voltage across output capacitor of dual active bridge DC-DC converter are high-frequency pulsating. Therefore, large capacitor is required to provide stable output voltage in the two kinds of DC-DC converters.

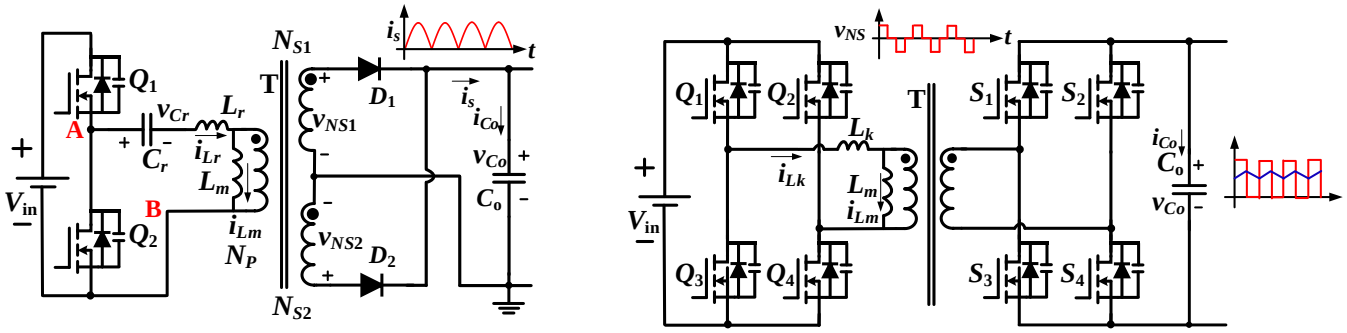

(a) *LLC* DC-DC converter in [34] (b) dual active bridge DC-DC converter in [21]

Fig. 15. Circuit diagram of the LLC DC-DC converter and dual active bridge DC-DC converter

In the proposed DCX, as shown in Fig. 10, if the leakage inductance of transformer, dead time and delay time as well as communication of switches are neglected, positive output voltage and negative output voltage are constant even without output capacitors because the driving signals of switches Q_1 and Q_2 are complementary with constant duty cycle 0.5 and the driving signals of switches S_1 and S_2 are complementary with constant duty cycle 0.5. The ideal equivalent circuit of the proposed DCX is shown in Fig. 16. The proposed DCX has smooth transition between positive and negative current i_{load} because input supply can be regarded as voltage source. When the switches and diodes are ideal, the leakage inductances and dead time t_{d1}~t_{d2} as well as delay time t_{d3}~t_{d4} are neglected, voltages v_{C3} and v_{C4} have no ripples. Then bipolar outputs voltage of the proposed DCX are

$$V_{C3} = -V_{C4} = \frac{nV_{in}}{2}. \tag{23}$$

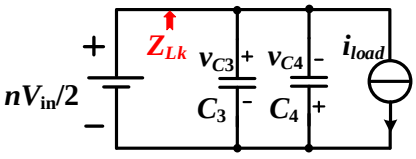

Fig. 16. Ideal equivalent circuit of the proposed DCX

In the proposed DCX, the leakage inductance L_{k2} is connected with diodes D_1 or D_2, and current i_{Lk2} has CCM and DCM due to complex AC load current of half bridge class-D audio amplifier. Generally, leakage inductances are small and have limited effect on outputs voltage gains. As shown in Fig. 17, simulation positive and negative outputs voltage gains are given with different leakage inductances and load current by PSIM software. According to equation (8), the equivalent load current of the proposed

DCX depends on modulation index m when $Z_{speaker}$=4Ω, φ=0, sin(ωt)=1 and V_{bus}=54V. It can be seen that outputs voltage gains can be regard as constant when leakage inductances are L_{k1}=L_{k2}=L_k=0.35μH.

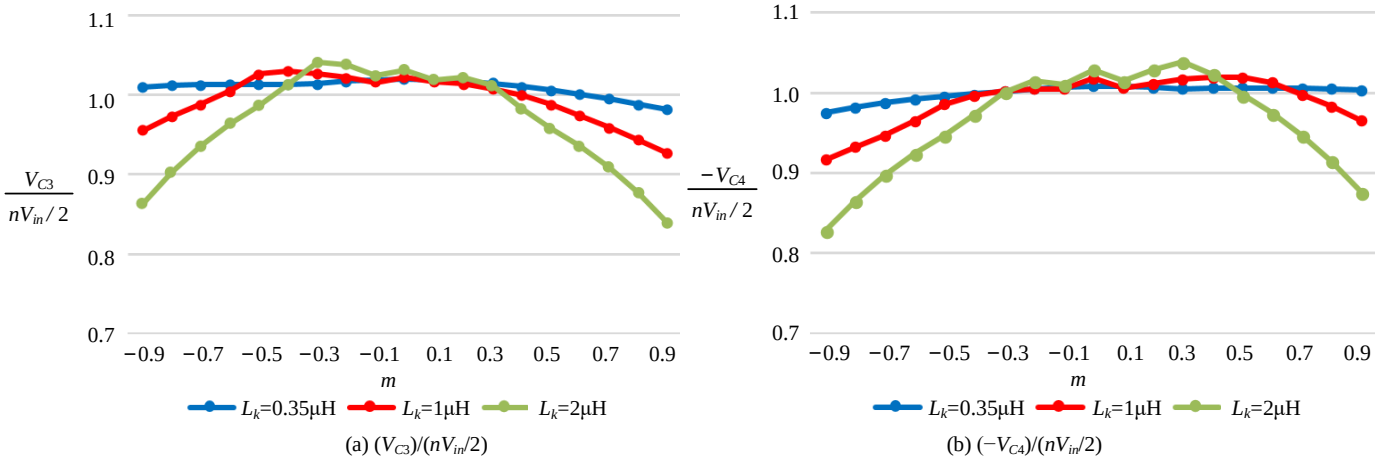

Fig. 17. Outputs voltage gains versus modulation index m under different L_{k1}= L_{k2}= L_k

The comparison between the proposed DCX and some other front-end DC-DC converters for class-D audio amplifier is summarized in Table I. It can be observed from Table I, the proposed DCX has simple controller, small output capacitors and soft switching of all the switches with bidirectional load current.

TABLE I

COMPARISON BETWEEN THE PROPOSED DCX AND SOME FRONT-END DC-DC CONVERTERS OF THE HALF-BRIDGE CLASS-D AUDIO AMPLIFIER

References	Flyback in [8]	VDRBHB in [10]	Bidirectional DC-DC converter in [17]	Bidirectional *LLC* converter in [28]	*LLC* DCX in [32]	*LLC* DCX in [34]	Proposed DCX
Switch	1	2	8	8	10	4	4
Diode	2	4	0	0	0	0	2
Inductor	0	2	1	2	0	1	0
Transformer	1	1	1	1	1	1	1
Controller	Complex	Complex	Complex	Complex	Simple	Simple	Simple
Output capacitor of the DC-DC converter	1000μF	470μF	-	-	-	440μF	20μF
Bidirectional power flowing	No	No	Yes	Yes	Yes	Yes	Yes
Soft switching in forward / backward mode	No / No	Yes / No	Yes / Yes	Yes / Yes	Yes / No	Yes / No	Yes / Yes
Input / output voltage	110V/48V	12V/±18V	500V/250V	75~130V/400V	380V/12V	400V/12V	311V/±54V
Switching frequency	25kHz	100kHz	100kHz	69kHz~92kHz	1MHz	530kHz	200kHz
Output power	100W	60W	1kW	1kW	800W	300W	200W
Efficiency	84.04%	88.3%	98.2%	97.1%	97.6%	97.7%	96.3%

IV. EXPERIMENTAL RESULTS

To verify the analysis results of the proposed DCX, a 200W prototype is implemented. The circuit diagram is shown in Fig. 18. Because in half bridge class-D audio amplifier system, the class-D audio amplifier is close-loop and has high PSRR, the proposed

DCX is open-loop and provide a probable bus voltage for the class-D audio amplifier. Thus, rectified line voltage is adopted as input power supply for the proposed audio amplifier system. In order to reduce the input voltage ripple, a smoothing capacitor C_{in} is parallel with rectified line voltage.

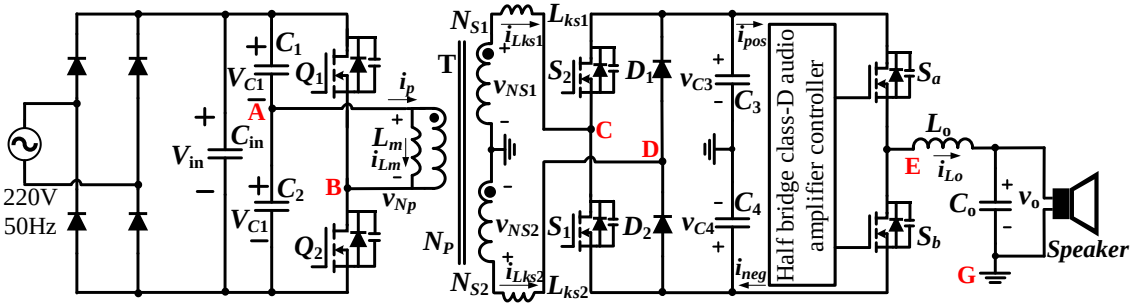

Fig. 18. Circuit diagram of the proposed half bridge class-D audio amplifier system

For 200W class-D audio amplifier system, when modulation index m=1, the minimum bus voltages of half bridge class-D audio amplifier should satisfy

$$\left(\frac{V_{C3,\min}}{\sqrt{2}}\right)^2 / R_{speaker} \geq P_{out}. \tag{24}$$

According to [37], the peak-peak ripple voltage across capacitor C_{in} is

$$\Delta V_{in,pp} = \frac{P_{out}}{2\sqrt{2} f_{in} C_{in} V_{ac}}. \tag{25}$$

When the input voltage is minimal, (24) should be satisfied. The minimal input voltage is

$$V_{in,\min} = (1-20\%)\cdot\sqrt{2}V_{ac} - \Delta V_{in,pp}/2. \tag{26}$$

When V_{ac}=220V, P_{out}=200W, $R_{speaker}$=4Ω, f_{in}=50Hz, from (23) and (24)-(26), it has

$$C_{in} > 198.04uF. \tag{27}$$

In this paper, C_{in}=220μF is selected.

The specifications and circuit parameters are given in TABLT II.

TABLE II
SPECIFICATIONS AND CIRCUIT PARAMETERS

Output power, P_o		200W
Input Voltage, V_{in} / Output Voltage, V_{out}		Nominal 311V / ±54V
Switching Frequency, f_s		200kHz
Capacitors C_{in}		220μF
Capacitors C_1-C_2 / C_3-C_4		1μF / 20μF
Dead time t_{d1}=t_{d2}/ delay time t_{d3}=t_{d4}		60ns / 100ns
Transformer	N_p : N_{S1}: N_{S2}	20: 7: 7

	Magnetizing inductance L_m	85.1μH
	Leakage inductances L_{ks1}=L_{ks2}=L_k (transferred to secondary side)	0.35μH
Primary side switches Q_1 and Q_2		FDPF20N50FT
Secondary side switches S_1 and S_2		TPH1500CNH
Secondary side diodes D_1 and D_2		ES3DB

Fig. 19(a) shows output voltage, positive and negative bus voltage of audio amplifier by using the converter in [10] as front-end DC-DC converter, with V_{pos}=−V_{neg}=34V, f_o=20Hz, R_{load}=8Ω, C_{pos}=C_{neg}=500μF and v_o=13.5V AC. It can be observed that the ripple of bus voltages is large.

Fig. 19(b) shows output voltage, positive and negative bus voltage of audio amplifier by using the proposed DCX as front-end converter, with V_{C3}=−V_{C4}=54V, R_{load}=8Ω, C_3 = C_4 = 20μF and v_o=13.5V AC. It can be observed that the ripple of the bus voltages in the proposed DCX is much smaller than that in [10]. The results verify that the proposed DCX eliminates the power supply pumping of half bridge class-D audio amplifier with small DCX output capacitors.

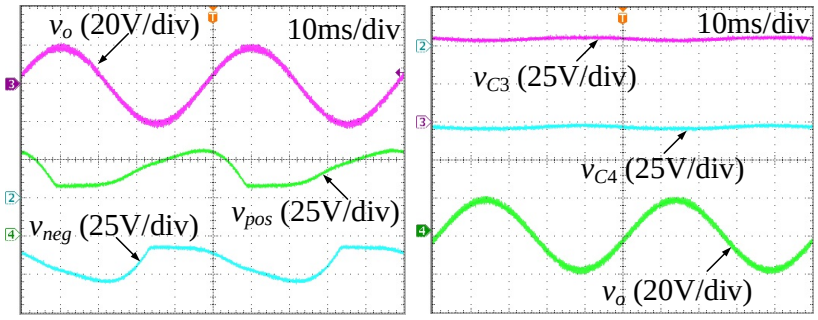

(a) (b)

Fig. 19. Experimental waveforms of positive and negative bus voltage and audio amplifier output voltage with 8Ω load (a) the unidirectional converter in [10] with V_{pos}= −V_{neg}=34V, f_o=20Hz, C_{pos}=C_{neg}=500μF and v_o=13.5V AC (b) the proposed DCX with V_{C3}=−V_{C4}=54V, f_o=20Hz, C_3=C_4=20μF and v_o=13.5V AC

Fig. 20(a) shows primary current i_p, positive and negative bus voltage V_{C3} and V_{C4}, and transformer primary voltage v_{AB} of the proposed DCX connected half bridge class-D audio amplifier. Fig. 20(b)-(d) show transformer primary voltage v_{AB} as well as currents i_{Lk1} and i_{Lk2}, when half bridge class-D audio amplifier operates at light load, positive heavy load and negative heavy load.

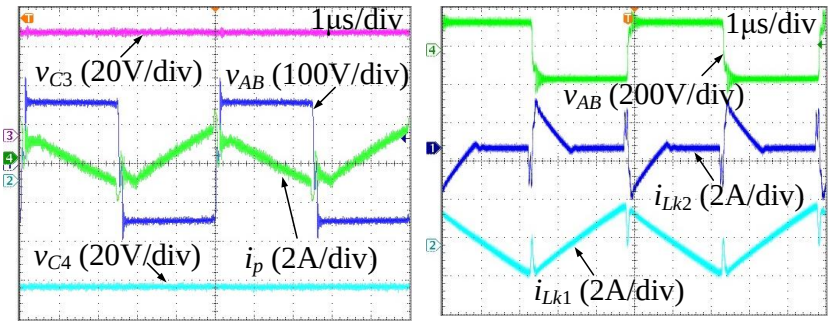

(a) (b)

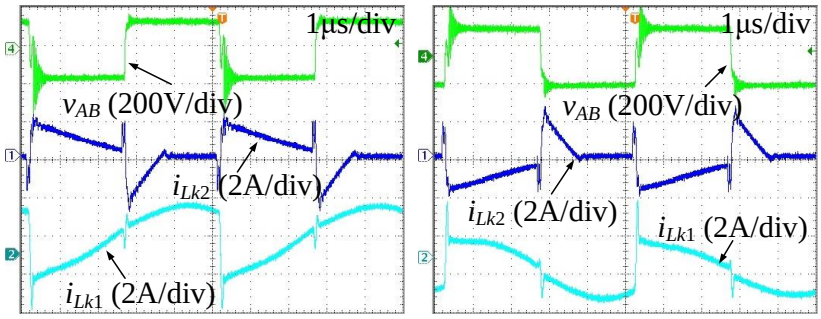

(c) (d)

Fig. 20. Experimental waveforms of the proposed DCX connected half bridge class-D audio amplifier (a) primary current i_p, positive and negative bus voltage V_{C3} and V_{C4}, and the voltage across transformer primary v_{AB} (b) currents i_{Lk1} and i_{Lk2} when the half bridge class-D audio amplifier is light load, and the voltage across transformer primary v_{AB} (c) currents i_{Lk1} and i_{Lk2} when the half bridge class-D audio amplifier is heavy load and load current i_{load} is positive, and the voltage across transformer primary v_{AB} (d) currents i_{Lk1} and i_{Lk2} when the half bridge class-D audio amplifier is heavy load and load current i_{load} is negative, and the voltage across transformer primary v_{AB}

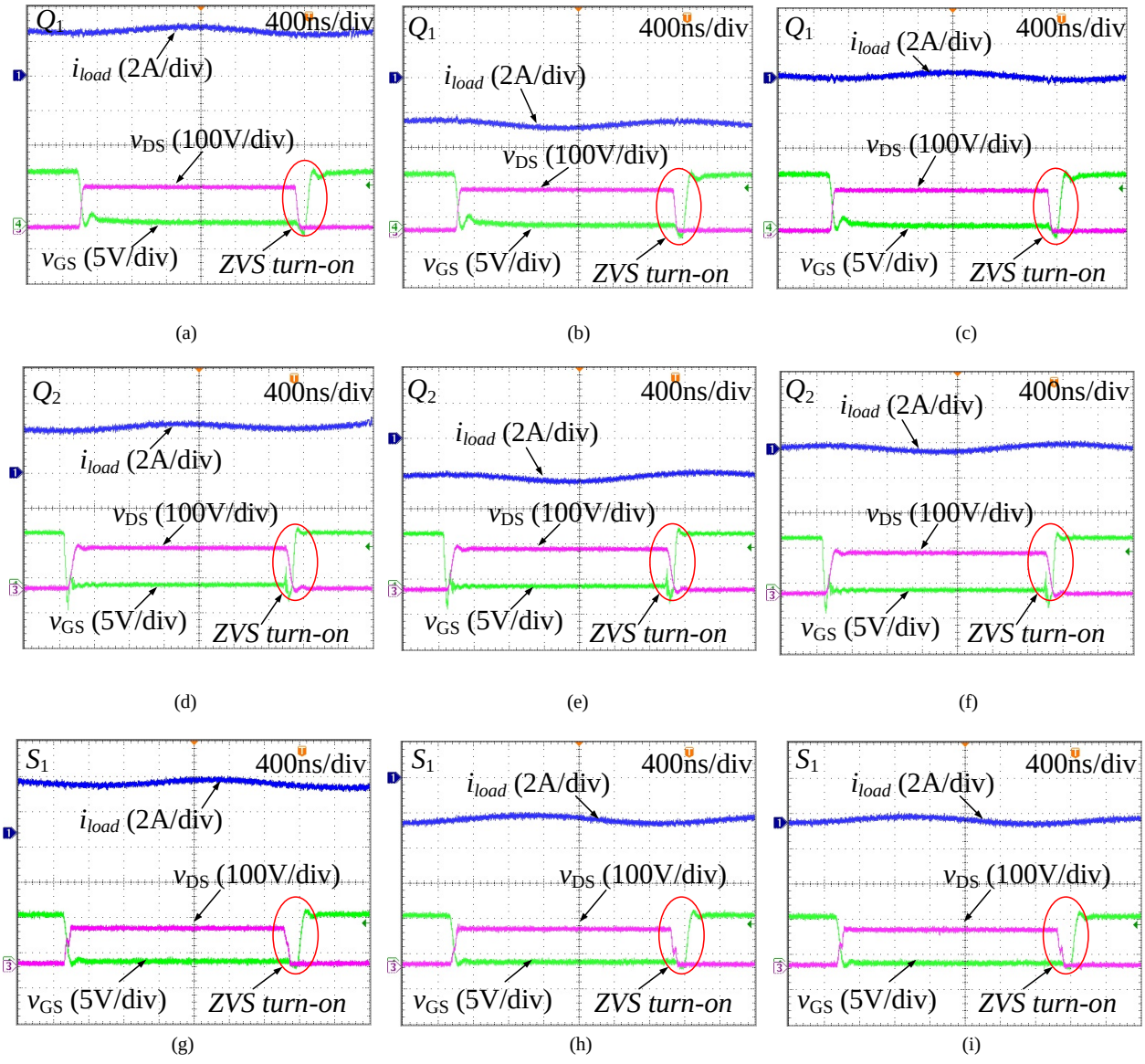

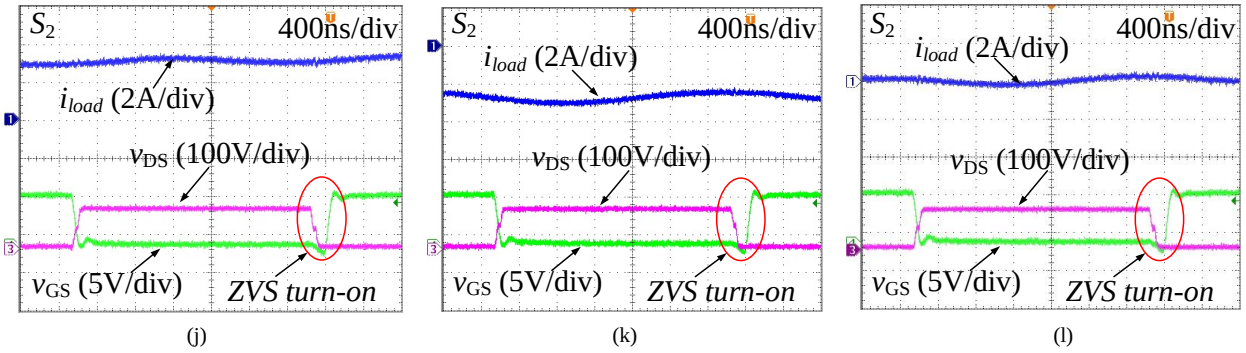

Fig. 21. Waveforms of v_{DS} and v_{GS} of MOSFETs in the proposed DCX

Fig. 21(a)-(l) show drain-source voltage V_{DS} and gate-source voltage V_{GS} of the MOSFETs in the proposed DCX when load current is positive, zero and negative. It can be observed that ZVS turn-on of switches Q_1-Q_2 and S_1-S_2 are realized.

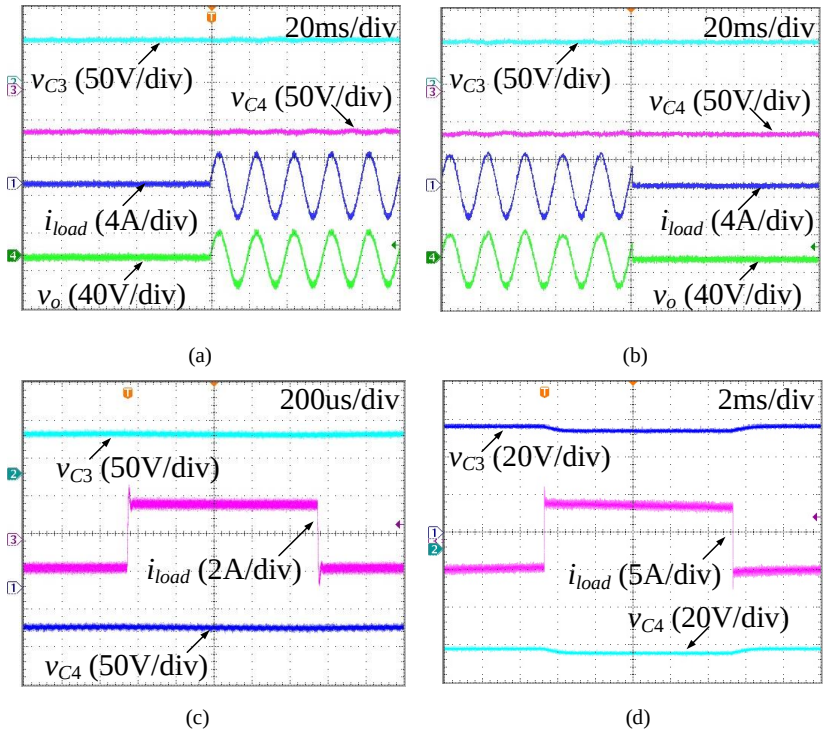

Fig. 22. Dynamic performance of the proposed DCX connected half bridge class-D audio amplifier with resistive load: (a) Step load increase from 0A to 2.5A for 50Hz sinusoidal audio amplifier output frequency. (b) Step load decrease from 2.5A to 0A for 50Hz sinusoidal audio amplifier output frequency. (c) Step load between 2A and -2A for 500Hz square audio amplifier output frequency (d) Step load between 4A and -4A for 50Hz square audio amplifier output frequency

Fig. 22(a)-(b) show dynamic performance of the proposed audio amplifier system with 8Ω resistive load, under step load variation from 0A to 2.5A, and from 2.5A to 0A, with the frequency of audio amplifier output sinusoidal voltage is 50Hz. As shown in Fig. 22(a)-(b), the output voltages of the proposed DCX are constant under step load variation of class-D audio amplifier, which reduces power supply pumping of half bridge class-D audio amplifier with small output capacitor of the DCX. Fig. 22(c) shows dynamic performance of the proposed audio amplifier system with 4Ω resistive load, under step load variation from -2A to 2A, and from 2A to -2A, with the frequency of audio amplifier output square voltage is 50Hz. Fig. 22(d) shows dynamic

performance of the proposed audio amplifier system with 4Ω resistive load, under step load variation from -4A to 4A, and from 4A to -4A, with the frequency of audio amplifier output square voltage is 50Hz. As shown in Fig. 22(c)-(d), the bipolar outputs voltages of the proposed DCX are smoothing and stable relatively.

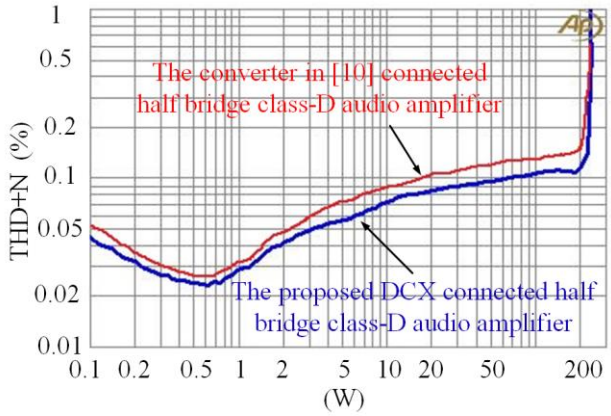

Fig. 23. The audio amplifier output voltage THD+N versus output power of the proposed DCX and the converter in [10] connected half bridge class-D audio amplifier

By using audio analyzer (Audio Precision 515), Fig. 23 shows the output voltage THD+N of the audio amplifier system with the proposed DCX and with the converter in [10] under different output power at 20Hz output voltage frequency with 4Ω resistor load. From Fig. 23, output voltage THD+N of half bridge class-D audio amplifier with the proposed DCX is lower than that with the converter in [10], because the proposed DCX eliminates the power supply pumping of the half bridge class-D audio amplifier.

Fig. 24 shows the measured efficiency of the proposed converter. It can be observed that the highest efficiency is 96.3% at 100W load, and the efficiency is higher than 95% over a wide load range. The proposed DCX idle loss is 2.15W, and class-D idle loss is 4.42W. Fig. 25 shows the prototype of the proposed DCX.

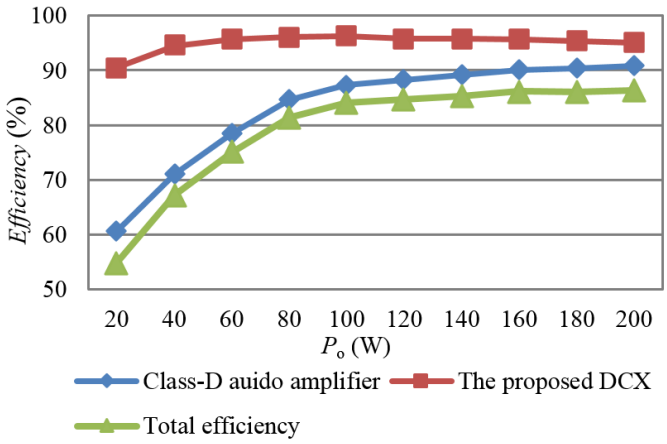

Fig. 24. Measured efficiency

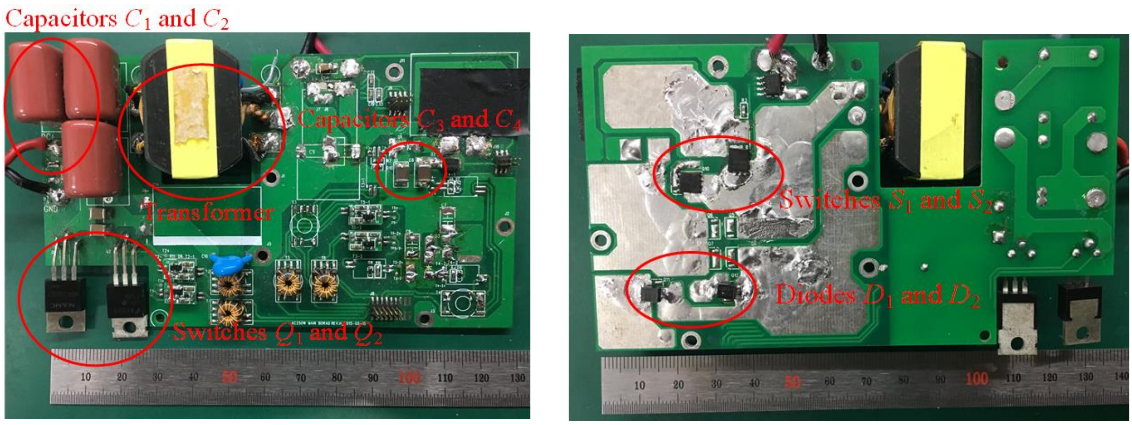

(a) Power board (Top) (b) Power board (Bottom)

Fig. 25. Prototype of the proposed DCX

V. CONCLUSION

A soft switching symmetric bipolar outputs DC-transformer (DCX) for eliminating power supply pumping of half bridge class-D audio amplifiers is proposed. Power supply pumping of half bridge class-D audio amplifier is eliminated by using the proposed DCX as front-end DC-DC converter. Compared with using bulk electrolytic capacitor to reducing the power supply pumping and voltage stress of half bridge class-D audio amplifier, the proposed DCX only need small output capacitors, and thus the power density of the audio amplifier system is improved. The proposed DCX provides stable symmetric bipolar output voltages bus with small switching ripple for half bridge class-D audio amplifier. In addition, the proposed DCX has smoothing transition between positive load current and negative load current with simple open-loop controller. ZVS turn-on of all the switches can be realized under AC load current, and thus high system efficiency is achieved in the proposed DCX.

REFERENCES

[1] Xicheng Jiang, "Fundamentals of audio class D amplifier design: a review of schemes and architectures," *IEEE Solid-State Circuits Magazine.,* vol. 9, issue. 3, pp. 14-25, 2017.

[2] Miguel Angel Rojas-González and Edgar Sánchez-Sinencio, "Low-power high-efficiency class D audio power amplifiers," *IEEE Journal of Solid-State Circuits.,* vol. 44, no. 12, pp. 3272-3284, Dec. 2009.

[3] IRAUDAMP7D: 25W-500W scalable output power class D audio power amplifier reference design using the IRS2092 protected digital audio driver. [Online]. Available: https://www.infineon.com.

[4] Bob Cordell, "Designing audio power amplifiers," New York: McGraw Hill, 2010: Chapter 29.5.

[5] Marco Berkhout, Lûtsen Dooper and Benno Krabbenborg, "A 4Ω 2.65W class-D audio amplifier with embedded dc-dc boost converter, current sensing ADC and DSP for adaptive speaker protection," *IEEE Journal of Solid-State Circuits.,* vol. 48, no. 12, pp. 2952-2961, Dec. 2013.

[6] Shin-Hao Chen, Kuei-Liang Lin, Shao Siang Ng, Tzu-Chi Huang, Ke-Horng Chen, Ying-Hsi Lin, Tsung-Yen Tsai and Chao-Cheng Lee, "Embedded single-inductor bipolar-output dc–dc converter in class-D amplifier for low common noise," *IEEE Transactions on Power Electronics,* vol. 31, no. 4, pp. 3106-3117, Apr. 2016.

[7] Xavier Branca, Bruno Allard, Xuefang Lin-Shi and David Chesneau, "Single-inductor bipolar-outputs converter for the supply of audio amplifiers in mobile platforms," *IEEE Transactions on Power Electronics,* vol. 28, no. 9, pp. 4248-4259, Sep. 2013.

[8] Ya-Jung Tu, Tai-Lang Jong, Chang-Ming Liaw, "Development of a class-D audio amplifier with switch-mode rectifier front-end and its waveform control," *IET power electronics.,* vol. 4, issue. 4, pp. 1002-1014, 2011.

[9] IRAUDPS3-30V: +/−30V power supply for class-D audio amplifier reference design user guide. [Online]. Available: https://www.infineon.com.

[10] Chong-Eun Kim, Gun-Woo Moon and Sang-Kyoo Han, "Voltage doubler rectified boost-integrated half bridge (VDRBHB) converter for digital car audio amplifiers," *IEEE Transactions on Power Electronics,* vol. 22, no. 6, pp. 2321-2330, Nov. 2007.

[11] Dennis Nielsen, "Class D audio amplifiers for high voltage capacitive transducers," Ph.D. dissertation, Technical University of Denmark, 2014.

[12] Self Douglas, "Audio power amplifier design," Taylor & Francis, 2013.

[13] Tong Ge and Joseph S. Chang, "Bang-bang control class D amplifiers: total harmonic distortion and supply noise," *IEEE Transactions on Circuits and Systems I: Regular Papers,* vol. 56, no. 10, pp. 2353–2361, Oct. 2009.

[14] Adrian Israel Colli-Menchi, Joselyn Torres and Edgar Sánchez-Sinencio, "A feed-forward power-supply noise cancellation technique for single-ended class-D audio amplifiers," *IEEE Journal of Solid-State Circuits.,* vol. 49, no. 3, pp. 718-728, Mar. 2014.

[15] Wei Shu and Joseph Sylvester. Chang, "Power supply noise in analog audio class D amplifiers," *IEEE Transactions on Circuits and Systems I: Regular Papers,* vol. 56, no. 1, pp. 84–96, Jan. 2009.

[16] Shu Zhong, Jianping Xu and Xiang Zhou, "2.1-channel switching amplifier with dc/high-frequency-ac mixed power supply for efficiency improvement and bus voltage pumping elimination," *IEEE Transactions on Power Electronics,* to be published, DOI 10.1109/TPEL.2018.2815742.

[17] Yanfeng Shen, Huai Wang, Ahmed Al-Durra, Zian Qin and Frede Blaabjerg, "A bidirectional resonant dc–dc converter suitable for wide voltage gain range," *IEEE Transactions on Power Electronics,* vol. 33, no. 4, pp. 2957-2975, Apr. 2018.

[18] Hongfei Wu, Shun Ding, Kai Sun, Li Zhang, Yuewei Li and Yan Xing, "Bidirectional soft-switching series-resonant converter with simple PWM control and load-independent voltage-gain characteristics for energy storage system in DC microgrids," *IEEE Journal of Emerging and Selected Topics in Power Electronics,* vol. 5, no. 3, pp. 995-1007, Sep. 2017.

[19] Hongfei Wu, Kai Sun, Yuewei Li and Yan Xing, "Fixed-frequency PWM-controlled bidirectional current-fed soft-switching series-resonant converter for energy storage applications," *IEEE Transactions on Industrial Electronics,* vol. 64, no. 8, pp. 6190-6201, Aug. 2017.

[20] Kang Xiangli, Shouxiang Li and Keyue Ma Smedley, "Decoupled PWM plus phase-shift control for a dual-half-bridge bidirectional dc-dc converter," *IEEE Transactions on Power Electronics,* to be published, DOI 10.1109/TPEL.2017.2758398.

[21] Biao Zhao, Qiang Song, Wenhua Liu and Yandong Sun, "Overview of dual-active-bridge isolated bidirectional DC–DC converter for high-frequency-link power-conversion system," *IEEE Transactions on Power Electronics,* vol. 29, no. 8, pp. 4091-4106, Aug. 2014.

[22] Zhiyuan Hu, Laili Wang, Hongliang Wang,Yan-Fei Liu and Paresh C. Sen, "An accurate design algorithm for *LLC* resonant converters—Part I," *IEEE Transactions on Power Electronics,* vol. 31, no. 8, pp. 5435-5447, Aug. 2016.

[23] Ho-Young Yoon, Hyeon-Seok Lee, Seok-Hyeong Ham, Hyung-Jin Choe, and Bongkoo Kang, "Off-time control of *LLC* resonant half-bridge converter to prevent audible noise generation at a light load condition," *IEEE Transactions on Power Electronics,* to be published, DOI 10.1109/TPEL.2017.2774840.

[24] Chao Fei, Qiang Li and Fred C. Lee, "Digital implementation of adaptive synchronous rectifier (SR) driving scheme for high-frequency *LLC* converters with microcontroller," *IEEE Transactions on Power Electronics,* vol. 33, no. 6, pp. 5351-5361, Jun. 2018.

[25] Chao Fei, Fred C. Lee and Qiang Li, "Digital implementation of soft start-up and short-circuit protection for high-frequency *LLC* converters with optimal trajectory control (OTC)," *IEEE Transactions on Power Electronics,* vol. 32, no. 10, pp. 8008-8017, Oct. 2017.

[26] Chao Fei, Yuchen Yang, Qiang Li and Fred C. Lee, "Shielding technique for planar matrix transformers to suppress common-mode EMI noise and improve efficiency," *IEEE Transactions on Industrial Electronics,* vol. 65, no. 2, pp. 1263-1272, Feb. 2018.

[27] Jee-Hoon Jung, Ho-Sung Kim, Myung-Hyo Ryu and Ju-Won Baek, "Design methodology of bidirectional *CLLC* resonant converter for high-frequency isolation of dc distribution systems," *IEEE Transactions on Power Electronics*, vol. 28, no. 4, pp. 1741-1755, Apr. 2013.

[28] Tianyang Jiang, Junming Zhang, Xinke Wu, Kuang Sheng and Yousheng Wang, "A bidirectional *LLC* resonant converter with automatic forward and backward mode transition," *IEEE Transactions on Power Electronics*, vol. 30, no. 2, pp. 757-770, Feb. 2015.

[29] Jiepin Zhang, Jianqiang Liu, Jingxi Yang, Nan Zhao, Yang Wang and Trillion Zheng, "A *LLC-LC* type bidirectional control strategy for *LLC* resonant converter in power electronic traction transformer," *IEEE Transactions on Industrial Electronics*, to be published, DOI 10.1109/TIE.2018.2808917.

[30] Chao Fei, Mohamed H. Ahmed, Fred C. Lee and Qiang Li, "Two-stage 48 V-12 V/6 V-1.8 V voltage regulator module with dynamic bus voltage control for light-load efficiency improvement," *IEEE Transactions on Power Electronics*, vol. 32, no. 7, pp. 5628-5636, Jul. 2017.

[31] Mohamed H. Ahmed, Chao Fei, Fred C. Lee and Qiang Li, "48-V voltage regulator module with PCB winding matrix transformer for future data centers," *IEEE Transactions on Power Electronics*, vol. 64, no. 12, pp. 9302-9310, Dec. 2017.

[32] Chao Fei, Fred C. Lee and Qiang Li, "High-efficiency high-power-density *LLC* converter with an integrated planar matrix transformer for high-output current applications," *IEEE Transactions on Industrial Electronics*, vol. 64, no. 11, pp. 9072-9082, Nov. 2017.

[33] Mingkai Mu and Fred C. Lee, "Design and optimization of a 380–12 V high-frequency, high-current *LLC* converter with GaN devices and planar matrix transformers," *IEEE Journal of Emerging and Selected Topics in Power Electronics*, vol. 4, no. 3, pp. 854-862, Sep. 2016.

[34] Weiyi Feng, Paolo Mattavelli and Fred C. Lee, "Pulsewidth locked loop (PWLL) for automatic resonant frequency tracking in *LLC* dc-dc transfo*rmer* (*LLC*-DCX)*," IEEE Transactions on Power Electronics*, vol. 28, no. 4, pp. 1862-1869, Apr. 2013.

[35] Wei Qin, Xinke Wu and Junming Zhang, "Current-feed single-switch forward resonant dc transformer (DCX) with secondary diode-clamping," *IEEE Transactions on Industrial Electronics*, vol. 64, no. 10, pp. 7790-7799, Oct. 2017.

[36] Wei Qin, Xinke Wu and Junming Zhang, "A family of dc transformer (DCX) topologies based on new ZVZCS cells with dc resonant capacitance," *IEEE Transactions on Power Electronics*, vol. 32, no. 4, pp. 2822-2834, Apr. 2017.

[37] Schäffer Johannes, "Rectifier circuits: theory and design.," New York: Wiley, 1965.